Exchange interactions of Er^{3+} in the *ab* plane for $Er_xY_{1-x}Ba_2Cu_3O_{7-\delta}$: An EPR linewidth study

V. Likodimos and N. Guskos*
Solid State Section, Department of Physics, University of Athens, 157 84 Zografos, Athens, Greece

H. Garmari-Seale
NCSR ''Democritos,'' Aghia Paraskevi Attikis 153 10, Athens, Greece

M. Wabia and J. Typek
Institute of Physics, Technical University of Szczecin, 70-310 Szczecin, Poland
(Received 13 February 1998; revised manuscript received 7 August 1998)

The electron paramagnetic resonance (EPR) linewidth of Er^{3+} in $Er_xY_{1-x}Ba_2Cu_3O_{7-\delta}$ ($\delta \approx 1$) is studied as a function of Er concentration. The EPR spectrum complies with the crystal-field ground doublet, while linewidth analysis shows the presence of exchange narrowing. Comparison of the theoretical EPR linewidth with the experimental data provide evidence for the presence of nearest-neighbor exchange interactions of the order of 1 K, most probably anisotropic along the *a* and *b* crystallographic axes. [S0163-1829(98)04345-8]

Numerous experimental studies have been devoted in the investigation of rare-earth (R) magnetism in $RBa_2Cu_3O_{7-\delta}$ high-T_c superconductors.[1] Theoretical calculations have shown that though the dipole-dipole interaction contributes significantly in the low-temperature ordered states of R^{3+} ions,[2] the transition temperatures calculated on the basis of the two-dimensional (2D) Ising dipolar model fall below the experimental values, indicating the presence of exchange coupling,[3] Analysis of the Gd^{3+} electron paramagnetic resonance (EPR) width has been employed to estimate the exchange interaction between Gd^{3+} spins (Refs. 4 and 5) and the weak coupling with charge carriers.[6,7]

Among the $RBa_2Cu_3O_7$ series, the Er-isostructural member presents particular interest since the Er^{3+} sublattice exhibits 2D Ising behavior below $T_N = 0.62$ K,[8] while the magnetic correlations exhibit substantial dependence on the oxygen content in $ErBa_2Cu_3O_{7-\delta}$.[9] Specific heat measurements have shown a substantial rounding of the transition for $\delta > 0.6$, which was described in terms of hybrids of 1D and 2D *XY* models.[10] Mössbauer and EPR experiments (Refs. 11 and 12) on Er-doped $YBa_2Cu_3O_{7-\delta}$ samples have consistently shown the Er^{3+} spectrum in reasonable agreement with the Kramers ground doublet predicted by crystal-field (CF) analysis of $ErBa_2Cu_3O_{7-\delta}$,[13] along with the presence of a molecular field due to the interaction of Er^{3+} with the Cu(2) planes. However, EPR measurements on $Er_xY_{1-x}Ba_2Cu_3O_6$ have shown the presence of two broad resonances which were interpreted as the result of two closely spaced ($\approx$1 K) doublets in the ground configuration of Er^{3+} ions.[14–16] In order to elucidate the origin of the EPR spectra and obtain information on the exchange coupling between Er^{3+} ions we have studied the Er^{3+} EPR spectrum in $Er_xY_{1-x}Ba_2Cu_3O_{7-\delta}$ ($\delta \approx 1$).

Oxygen deficient $Er_xY_{1-x}Ba_2Cu_3O_{7-\delta}$ ($x = 0.5, 1.0$) polycrystalline samples were as previously prepared.[17] Powder x-ray diffraction showed that the samples were single phase and had tetragonal crystal structure with lattice constants indicating a high degree of oxygen deficiency ($\delta > 07$). Magnetic measurements were performed with a PAR 155 VSM, while EPR measurements were carried out using an *X*-band Bruker 200D spectrometer, with an Oxford flow-cryostat for temperature-dependent measurements.

The inverse magnetic susceptibility $1/\chi$ vs T and magnetization $M(H)$ of $ErBa_2Cu_3O_{7-\delta}$ are shown in Fig. 1. The CF parameters for Er^{3+} ions in $ErBa_2Cu_3O_{7-\delta}$ have been determined by inelastic neutron scattering experiments.[13,18] The magnetic susceptibilities and magnetization, parallel and perpendicular to the *c* axis and their average values, were calculated from the reported CF parameters for $\delta = 0.66$ and $\delta = 0.91$. The corresponding average $1/\chi$ and $M(H)$ curves, which are practically identical, are in close agreement with

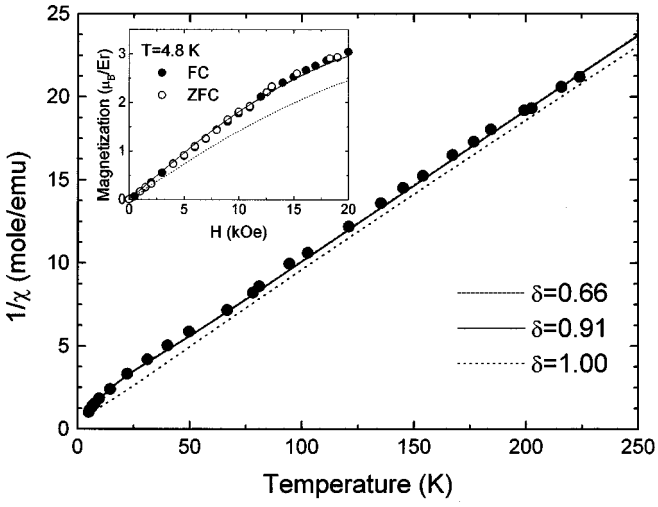

FIG. 1. Inverse magnetic susceptibility $1/\chi$ vs T (circles) for oxygen-deficient $ErBa_2Cu_3O_{7-\delta}$ at $H = 10$ kOe. The inset shows the $M(H)$ curves at $T = 4.8$ K in the ZFC and FC modes. The lines correspond to the average curves calculated according to the CF parameters of Ref. 13, $\delta = 0.66$ (dashed line), $\delta = 0.91$ (solid line) and Ref. 16, $\delta = 1.0$ (dotted line).

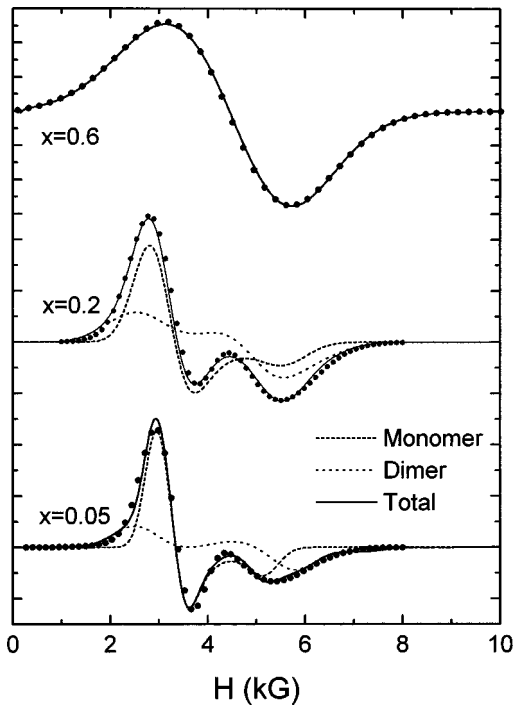

FIG. 2. EPR spectra of $Er_xY_{1-x}Ba_2Cu_3O_6$ (circles) ($x=0.6,0.2,0.05$) in the first derivative mode at $\nu_c=36.5$ GHz and $T=1.3$ K (Ref. 16). Solid lines correspond to the simulated Er^{3+} EPR spectra. Dotted and short-dashed lines correspond to the dimer and monomer EPR spectra.

the experimental data confirming the CF energy scheme (Fig. 1). However, based on the analysis of the Er^{3+} EPR results it was shown that a modification of the CF parameters derived from neutron scattering, mainly a reduction of B_2^0, results in two lowest lying, Γ_6 and Γ_7, doublets only 3 K apart in energy,[16] in contradiction with the neutron results predicting an energy gap of $\approx$80 K.[13] Calculation of $\chi(T)$ and $M(H)$ using the CF parameters from Ref. 16 results in significant discrepancy between the theoretical and experimental data (Fig. 1), most pronounced in the $M(H)$ curve which at $T=4.8$ K reflects the contribution of the lowest CF levels. Moreover, the latter CF parameters predict the c axis as the easy axis of magnetization contrary to other experimental results.[8,9]

The EPR spectra recorded soon after the preparation comprised the contribution of intense EPR spectra arising from copper clusters whose intensity was substantially reduced after storage of the samples at room temperature for 70 days. In that case the EPR spectrum is dominated by a very intense broad signal extending to the whole scan range having its maximum near zero magnetic field. Accurate fitting of the broad EPR signal is performed assuming the superposition of two Gaussian lines taking into account both absorptions at $+H_r$ and $-H_r$ induced by the two oppositely rotating components of the linearly polarized rf field. The resulting g values are found to be $g_1\approx 4$ and $g_2\approx 8$ for both samples, while the integral intensity $I(T)$ follows an $1/T$ law implying a paramagnetic center with spin $S=\frac{1}{2}$. Using the CF parameters for $ErBa_2Cu_3O_{7-\delta}$ that predict a Γ_7 ground doublet for $\delta=0.91,0.66$ and a Γ_5 one for $\delta\geqslant 0.55$,[13] the calculated g values along the principal a,b,c axes turn out to be close to the g_1, g_2 values of the experimental EPR spectrum allowing its identification with the axial powder EPR spectrum of Er^{3+} ions.

The broad EPR signal is very similar to the Er^{3+} resonance previously recorded for $ErBa_2Cu_3O_6$ powder samples at the X band, whose absorption profile has been almost fully detected at higher frequencies where the zero-field absorption was severely reduced.[14] The EPR absorption was interpreted in terms of the line shape function derived by Kubo and Toyabe (KT) for slowly fluctuating random fields of comparable or larger magnitude than the Zeeman field.[19] Fitting the EPR absorption with the superposition of two KT lines and noting the inability to fit the EPR spectra with an axial powder pattern, it was suggested that the Er^{3+} EPR resonance results from two closely spaced doublets which mix as the magnetic field is applied.[15] This suggestion was later corroborated by single crystal EPR measurements which showed the presence of two EPR lines independently on the orientation of the applied field.[16]

Subsequently, we attempted to simulate the high-frequency (35 GHz) Er^{3+} EPR spectra which were reconstructed on the basis of the two-KT line model and the reported EPR parameters (Ref. 16) using the MONOQF program (Ref. 20) with an axial powder spectrum and $g_\perp > g_\parallel$ as required by the anisotropy of the CF ground state. Hyperfine structure corresponding to the ^{167}Er isotope ($I=\frac{7}{2}$, 22.94%) was also included. For $x=1.0,0.8$ the EPR spectra could not be accurately simulated with $g_\perp > g_\parallel$ that may be due to the effect of the large zero-field absorption which was not taken into account by the line shape functions and/or to the contribution of clusters formed at low temperatures where the Er^{3+} magnetic correlations become effective. However, for $x=0.6$ quite satisfactory simulation (Fig. 2) is obtained for an axial EPR powder spectrum (Table I), though the g anisotropy is smaller than that predicted by the CF analysis. For lower Er concentrations ($x=0.2,0.05$), it has been observed

TABLE I. EPR parameters derived from the simulation of the Er^{3+} EPR spectra in $Er_xY_{1-x}Ba_2Cu_3O_6$ ($x=0.6,0.2,0.05$). The theoretical, dipolar, and exchange-narrowed EPR linewidths (in MHz) for H parallel to the c ($\Delta H_\parallel$) and a ($\Delta H_\perp$) axes, the latter derived for $J_a/k_B\approx 1.8$ K and $J_b/k_B\approx -0.85$ K, are included.

			Simulated				Theoretical			
x	$g_\parallel$	$g_\perp$	$A_\parallel$ (10^{-4} cm^{-1})	$A_\perp$ (10^{-4} cm^{-1})	$\Delta H_\parallel$ (MHz)	$\Delta H_\perp$ (MHz)	$\Delta H_d^{(\parallel)}$ (MHz)	$\Delta H_d^{(\perp)}$ (MHz)	$\Delta H_\parallel$ (MHz)	$\Delta H_\perp$ (MHz)
0.6	6.7	5.02	230	170	6000	11500	9560	22700	6000	11500
0.2	8.40	4.70	290	165	2800	4600	5500	13100	3200	5500
0.05	8.31	5.08	280	175	1800	2500	2760	6550	1250	3200

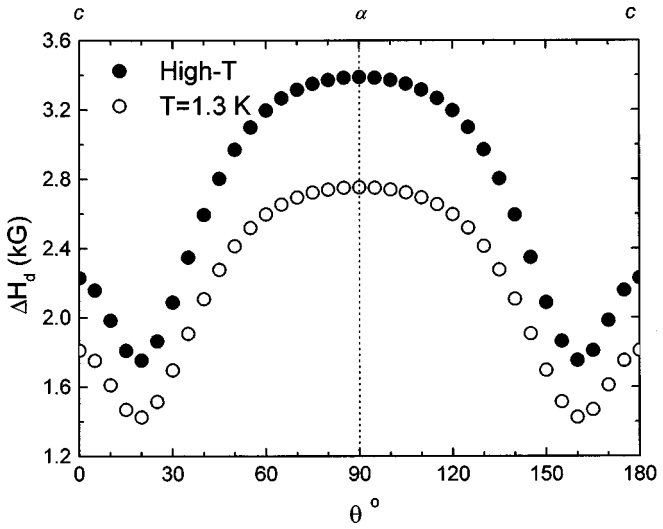

FIG. 3. Angular dependence of the dipolar width ΔH_d in the *ac* plane for $ErBa_2Cu_3O_{6.09}$ in the high-temperature approximation (solid circles) and at $T=1.3$ K (open circles).

that though the EPR spectra resemble the profile of an axial powder pattern, the relative weight of the parallel to the perpendicular component does not comply with that anticipated for axial symmetry (Fig. 2), indicating the presence of an additional contribution. In this case, Er^{3+} dimers appear as the most plausible candidate for such a contribution. Indeed, satisfactory simulation of the EPR spectra for $x=0.2,0.05$ is obtained using the superposition of the axial powder spectrum of single Er^{3+} ions (monomers) with the powder spectrum of Er^{3+} pairs (dimers) comprising two adjacent ions in the *ab* plane coupled by dipolar and exchange interactions (Fig. 3). The parameters for the monomer Er^{3+} EPR spectra are shown in Table I. For the simulation of the dimer EPR spectra performed with the GNDIMER program,[20] we have considered a pair of nearest-neighbor (NN) Er^{3+} ions in the *ab* plane with identical *g* and *A* tensors, namely, $g_\perp=7.0$, $g_\parallel=4.5$, $\Delta H_\perp=550$ G, $\Delta H_\parallel=500$ G and $g_\perp=7.0$, $g_\parallel=4.1$, $\Delta H_\perp=\Delta H_\parallel=400$ G for $x=0.2$ and $x=0.05$, respectively, with internuclear distance of one lattice constant ($r=3.85$ Å) and AFM isotropic exchange of -0.5 cm^{-1}, though it should be noted that the powder pattern does not exhibit substantial dependence on the exchange constant.

On the other hand, the EPR spectra for $ErBa_2Cu_3O_6$ single crystals prepared by annealing in vacuum, exhibited an intriguing two-line behavior rather than the angular variation of a uniaxial EPR spectrum, while a dependence of the EPR spectrum on the annealing conditions was also reported.[16] The single-crystal EPR data, especially for $H\perp c$, revealed two broad transitions which can be shown to be close to those expected for Er^{3+} dimers, further implying an increase of the Er^{3+} exchange interaction. Such an effect reminds us of the chemical preparation dependence that the Gd^{3+} EPR spectrum exhibited in $GdBa_2Cu_3O_7$ single crystals.[4] In particular, for a certain single crystal preparation, considerable narrowing of the EPR linewidth and suppression of its angular dependence were reported, suggested to arise from an enhanced exchange interaction between Gd^{3+} ions.[4] In this context, we may conclude that the Er^{3+} EPR spectrum in $Er_xY_{1-x}Ba_2Cu_3O_6$ is consistent with the CF ground doublet, though the resolution of ambiguities regarding the EPR spectra near the magnetic correlation regime and their dependence on δ and Er concentration, require further experimental work.

Furthermore, the EPR linewidth, which at low temperatures comprises negligible contributions either from spin-lattice or Korringa-like relaxation,[12,21] is analyzed employing the method of moments.[22] The secular second and fourth moments due to the dipole-dipole interaction as a function of the angle θ of *H* with the *c* axis and the Er concentration (x) have been calculated in the high-temperature approximation applying standard procedures.[22–24] In these derivations we have taken into account explicitly the axial *g* tensor of Er^{3+} ions, while due to the relatively large distance between the *R* layers along the *c* axis ($c\sim 3a$) in the $RBa_2Cu_3O_6$ structure, we have considered only Er^{3+} ions lying in the same *ab* plane with $a=b$. At low temperatures, where the Zeeman energy becomes comparable to the thermal energy, the high-temperature approximation ceases to be valid and the expected reduction of the second moment has been estimated to be 0.66 of the secular value for $\nu_c=36.5$ GHz and $T=1.3$ K.[25] The resulting dipolar width as a function of θ, $\Delta H_d(\theta)$, in the *ac* plane for $ErBa_2Cu_3O_6$ indicates the presence of considerable anisotropy (Fig. 3). Comparison of ΔH_d with the experimental linewidths (Table I) shows that the latter are much smaller than the theoretically predicted dipolar widths, indicating that exchange narrowing is effective.[26]

Next, we consider the exchange interaction between Er^{3+} spins expressed by $H_{\rm ex}=\Sigma_{j,k}J_{jk}S_j\cdot S_k$ with J_{jk} being the isotropic exchange coupling constant between two NN effective spins *j* and *k*. Although, the assumption of isotropic exchange interaction is arguable due to the orbital contribution in the rare earth ground state,[25] we assumed an effective isotropic exchange coupling between Er^{3+} spins (Refs. 3 and 10) allowing for different values, J_a and J_b along the *a* and *b* axes. The contribution of exchange to the secular fourth moment $M_{4,\rm ex}^{(0)}$ has been explicitly calculated allowing for the axial *g*-tensor and different coupling constants along the *a* and *b* axes. Analysis of the EPR linewidths for $x=0.6$ shows that $\nu_{\rm ex}$ is comparable or even larger than the Zeeman frequency $\nu_c=36.5$ GHz, indicating the intermediate exchange narrowing regime ($\nu_{\rm ex}\approx\nu_c$) where a frequency-dependent linewidth is expected.[27] Calculating the nonsecular contributions and following the frequency dependence of M_2 predicted by Kubo and Tomita,[27] we find the second moment parallel and perpendicular to the *c* axis, to be increased by $M_{2\perp}\approx 1.2M_{2\perp}^{(0)}$ and $M_{2\parallel}\approx 2.0M_{2\parallel}^{(0)}$, leading to $M_{2\perp}=7.52\times 10^8 x$ $(\rm MHz)^2$ and $M_{2\parallel}=2.16\times 10^8 x$ $(\rm MHz)^2$. Assuming the same frequency and temperature dependence for the second and fourth moment,[28] the values for the μ ratios are

$$\mu_{d\perp}=2.1+\frac{0.67}{x},\quad \mu_{d\parallel}=1.5+\frac{0.29}{x},$$

$$\mu_{\rm ex\perp}=(8.33J_a^2+10.67J_b^2-5.07J_aJ_b-46000J_a-26233J_b)(10^{-9}\ \rm MHz^2),$$

$$\mu_{\rm ex\parallel}=(17.78J_a^2+17.78J_b^2+6.94J_aJ_b-115200J_a-115200J_b)(10^{-9}\ \rm MHz^2), \quad (1)$$

with $\mu_d = M_{4,d}/M_{2,d}^2$ and $\mu_{ex} = M_{4ex}/M_{2,d}^2$. The calculated μ values do not satisfy the $\mu \gg 3$ condition required for Lorentzian line shape and thus we make use of the formula $\Delta H = \sqrt{\pi/2}(M_2/\mu - 1.87)^{1/2}$, covering the transition from the Gauss to Lorentz line shape according to the value of μ,[5] in accordance with the improved simulation of the EPR spectra with Gaussian line shape. Applying this relation along with the ΔH values determined for $x = 0.6$, we find $\mu_{2\perp} = 7.22$ and $\mu_{2\parallel} = 7.53$. Then, using Eqs. (1) and the latter values for μ defined as $\mu = \mu_d + \mu_{ex}$, the exchange constants are evaluated. If the exchange coupling constants are confined to be equal ($J_a = J_b = J$), we find two different AFM solutions ($J > 0$), namely $J = 24220$ MHz$\approx$1.2 K and $J = 29620$ MHz $\approx$1.4 K. The discrepancy between the two values can be attributed either to the approximation involved in the linewidth analysis, or to the inherent inadequacy of the physical assumption of isotropic exchange interactions.

If the exchange coupling constants are considered to be different, four sets of (J_a, J_b) roots are obtained, namely, (37500,$-$17720), (14430,$-$34470), ($-$33800,18050), ($-$3065,40150) in MHz, with the minus sign corresponding to the FM interaction. The first set, which corresponds to $J_a/k_B \approx 1.8$ K (AFM) and $J_b/k_B \approx -0.85$ K (FM) compares favorably with the magnetic ordering in $ErBa_2Cu_3O_{7-\delta}$, namely, FM chains of Er spins along the *b* axis with adjacent chains in the *ab* plane coupled antiferromagnetically.[8,9] The magnitude and the anisotropy of J_a/J_b are also in agreement with the interaction constants of the 1D and 2D *XY* models used to describe the specific heat behavior.[10] Calculation of the low-temperature ordered states for Er^{3+} (Ref. 2) using the latter J_a, J_b values shows that the $q(8y)$ configuration corresponding to the observed magnetic structure of the Er^{3+} sublattice becomes the lowest in energy, rather than the $q(6x)$ one predicted by the dipolar contribution, which corresponds to a reversal of the magnetic coupling in the *ab* plane. The latter result cannot be reproduced on the basis of the $J_a = J_b$ concept, thus supporting the presence of anisotropic exchange coupling along the *a* and *b* axes.

The derived J_a, J_b values can be used to predict the concentration dependence of the Er^{3+} EPR linewidth. The discrepancy between the theoretical and the experimental values for $x = 0.2, 0.05$ (Table I) is not very large if we take into account the approximate simulation of the latter EPR spectra and the possibility that for low Er concentrations the EPR linewidth may comprise a substantial contribution due to the fluctuations of the adjacent Cu(2) planes.[11,12]

We wish to thank Professor J. R. Pilbrow for the simulation programs and Dr. V. Petrouleas for arranging the EPR measurements.

*Author to whom correspondence should be sent. FAX: (+301)7257689; electronic address: ngouskos@atlas.uoa.gr

[1] J. W. Lynn, J. Alloys Compd. **181**, 419 (1992).
[2] S. K. Misra and J. Felsteiner, Phys. Rev. B **46**, 11 033 (1992).
[3] A. B. MacIsaak, J. P. Whitehead, K. de Bell, and K. S. Narayanan, Phys. Rev. B **46**, 6387 (1992).
[4] A. Deville, L. Bejjit, B. Gaillard, J. P. Sorbier, O. Monnereau, H. Noel, and M. Potel, Phys. Rev. B **47**, 2840 (1993).
[5] C. Fillip, C. Kessler, F. Balibanu, P. Kleeman, A. Darabont, L. V. Giurgiu, and M. Mehring, Physica C **235-240**, 1645 (1994); Physica B **222**, 16 (1996).
[6] D. Shaltiel, C. Noble, J. Pilbrow, D. Hutton, and E. Walker, Phys. Rev. B **53**, 12 430 (1996).
[7] C. Kessler, M. Mehring, P. Castellaz, G. Borodi, C. Filip, A. Darabont, and L. V. Giurgiu, Physica B **229**, 113 (1997).
[8] J. W. Lynn, T. W. Clinton, W.-H. Li, R. W. Erwin, J. Z. Liu, K. Vandervoort, and R. N. Shelton, Phys. Rev. Lett. **63**, 2606 (1989).
[9] H. Maletta, E. Porschke, T. Chattopadhyay, and P. J. Brown, Physica C **166**, 9 (1990).
[10] S. Simizu, G. H. Bellesis, J. Lukin, S. A. Friedberg, H. S. Lessure, S. M. Fine, and M. Greenblatt, Phys. Rev. B **39**, 9099 (1989).
[11] J. A. Hodges, P. Bonville, P. Imbert, and G. Jehanno, Physica C **184**, 283 (1991).
[12] I. N. Kurkin, I. Kh. Salikhov, L. L. Sedov, M. A. Teplov, and R. S. Zhdanov, JETP **76**, 657 (1993).
[13] J. Mesot, P. Allenspach, U. Staub, A. Furrer, H. Mutka, R. Osborn, and A. D. Taylor, Phys. Rev. B **47**, 6027 (1993).
[14] M. X. Huang, E. M. Jackson, S. M. Bhagat, L. Gupta, A. K. Rajarajan, and R. Vijayraghavan, J. Magn. Magn. Mater. **97**, 297 (1991).
[15] M. X. Huang, J. Barak, S. M. Bhagat, L. Gupta, A. K. Rajarajan, and R. Vijayraghavan, J. Appl. Phys. **70**, 5774 (1991).
[16] M. X. Huang, J. Barak, S. M. Bhagat, and J. L. Peng, J. Magn. Magn. Mater. **117**, 195 (1992).
[17] V. Likodimos, N. Guskos, H. Gamari-Seale, A. Koufoudakis, M. Wabia, J. Typek, and H. Fuks, Phys. Rev. B **54**, 12 342 (1996).
[18] L. Soderholm, C.-K. Loong, and S. Kern, Phys. Rev. B **45**, 10 062 (1992).
[19] R. Kubo and T. Toyabe, in *Magnetic Resonance and Relaxation*, edited by R. Blinc (North-Holland, Amsterdam, 1967), p. 810.
[20] J. R. Pilbrow, *Transition Ion Electron Paramagnetic Resonance* (Clarendon, Oxford, 1990).
[21] H. Shimizu, K. Fujiwara, and K. Hatada, Physica C **282-287**, 1349 (1997).
[22] J. H. Van Vleck, Phys. Rev. **74**, 1168 (1948).
[23] C. Kittel and E. Abrahams, Phys. Rev. **90**, 238 (1953).
[24] Z. G. Soos, K. T. McGregor, T. T. P. Cheung, and A. J. Silverstein, Phys. Rev. B **16**, 3036 (1977).
[25] J. M. Baker, Rep. Prog. Phys. **34**, 109 (1971).
[26] P. W. Anderson and P. R. Weiss, Rev. Mod. Phys. **25**, 269 (1953).
[27] R. Kubo and K. Tomita, J. Phys. Soc. Jpn. **9**, 888 (1954).
[28] J. E. Gulley, D. Hone, D. J. Scalapino, and B. G. Silbernagel, Phys. Rev. B **1**, 1020 (1970).